GPU Implementation of Oscillator Network System with Plastic Coupling for Dynamic Image Segmentation

Ken'ichi Fujimoto[1], Mio Kobayashi[2], Tetsuya Yoshinaga[1]
[1]Institute of Health Biosciences
The University of Tokushima, Japan
[2]Department of Systems and Control Engineering
Anan National College of Technology, Japan
{fujimoto, yosinaga}@medsci.tokushima-u.ac.jp, kobayashi@anan-nct.ac.jp

***ABSTRACT*:** *Image segmentation is a fundamental technique in image processing systems such as a medical computer-aided-diagnosis system. We previously proposed a discrete-time oscillator network system with a degradation (posterization) system for dynamic image segmentation. This system can extract image regions with similar pixel values (connected components) from a given gray-scale image and exhibit extracted image regions in a time series. The dynamics of the proposed system is described by ordinary difference equations. In spite of discrete-time system, our oscillator model can generate oscillatory responses like relaxation oscillations observed in ordinary differential equations. Dynamic image segmentation for a gray-scale image is performed according to posterization of pixel values and the synchronization of oscillatory responses from discrete-time oscillators. Since numerical integration is unnecessary to work the proposed system, its processing speed is significantly faster than that of another dynamic image-segmentation system consisting of ordinary differential equations. In this paper, for further speed-up of dynamic image-segmentation processing, we presented an implementation of the proposed system into a graphics processing unit.*

Keywords: Discrete-time Oscillator Network, Dynamic Image Segmentation, Graphics Processing Unit, Plastic Coupling, Synchronization

Received: 1 November 2012, Revised 17 December 2012, Accepted 22 December 2012

1. Introduction

Image segmentation is key technique in various image-processing systems such as a computer-aided-diagnosis system [1] for medical images. Many frameworks for image segmentation have been proposed [2, 3].

A locally-excitatory globally-inhibitory oscillator network (LEGION) [4] described by ordinary differential equations can extract image regions (connected components) from a given image and exhibit extracted image regions in a time series according to the synchronization of oscillators. We call this function "*dynamic image segmentation*". A LE- GION is novel but needs a huge computational cost to perform dynamic image segmentation because of numerical integration.

In contrast, we previously proposed a discrete-time oscillator network system for dynamic image segmentation [5, 6, 7, 8, 9]. In spite of discrete-time system, the proposed oscillator can generate oscillatory responses like relaxation oscillations observed in ordinary differential equations. Since numerical integration is unnecessary to work the proposed system, the processing of dynamic image-segmentation is quite faster than that of LEGIONs. To improve the proposed dynamic image-segmentation

system, on the basis of nonlinear control theory, we constructed a control system [10] for preventing the generation of a fixed point that corresponds to non-oscillatory responses and is unsuitable for dynamic image segmentation. Moreover, we proposed a method [11] to identify target image regions for a given binary (black and white) image using bifurcation theory. This supports that we know the number of image regions to be segmented before the process of image segmentation.

For segmenting continuous-tone gray-scale images, we also proposed an extended discrete-time oscillator network with a degradation (posterization) system [12]. In this system, couplings between neighboring oscillators can change every discrete time. The updating of coupling strengths is based on the dynamics of a posterization system that is modified from a discrete-time system [13]. We demonstrated that the extended dynamic image-segmentation system worked well for continuous-tone gray-scale images [12].

For further speed-up of dynamic image-segmentation processing, we previously implemented a small-size discrete time oscillator network into a field-programmable gate array (FPGA) [14]. However, its implementation not only requires a special device but also the implementation of a large-size oscillator network system is difficult. In contrast, a graphics processing unit (GPU) that can be mounted with personal computers (PCs) is available for PC end-users and can be process a large-size oscillator network system. In this paper, we present an implementation of our extended dynamic image-segmentation system [12] into a GPU and compare the amount of time required to segment continuous- tone gray-scale images on a GPU and a central processing unit (CPU).

2. System Description

2.1 Discrete-time Oscillator Network

As illustrated in Figure 1, our discrete-time oscillator network for segmenting a given *N*-pixel image consists of *N* discrete-time oscillators and a global inhibitor. All the oscillators are arranged in a grid so that an oscillator corresponds to a pixel.

The i^{th} oscillator has two internal variables (x_i, y_i) and its dynamics is described by

$$x_i(t+1) = k_f x_i(t) + d_i(t) + W_x \cdot W_i^S(t) \cdot g(x_i(t) + y_i(t), \theta_c) - W_z \cdot g(z(t), \theta_z) + C_i^x(t) \quad (1)$$

$$y_i(t+1) = k_r y_i(t) + \alpha \cdot g(x_i(t) + y_i(t), \theta_c) + a + C_i^y(t) \quad (2)$$

and the dynamics of the global inhibitor is defined by

$$z(t+1) = \phi \left\{ g\left(\sum_{k=1}^{N} g(x_k(t) + y_k(t), \theta_f), \theta_d \right) - z(t) \right\} \quad (3)$$

In (1) – (3), $g(.,.)$ is the output function of an oscillator and a global inhibitor. It is defined as

$$g(u(t)\theta) = \frac{1}{1 + \exp(-(u(t) - \theta)/\varepsilon)} \quad (4)$$

where $u(t)$ corresponds to the value of internal states and represents the threshold.

In (1), $d_i(t)$ represents the external input that takes a value from zero to two, which is directly proportional to the i^{th} posterized pixel value. An oscillator has two self-feedback inputs, and W_x and denote the time-invariant self- feedback strength. The self-feedback in (2) always exists, but the other in (1) is formed only when the value of $d_i(t)$ is high so that the ith pixel value is higher than , which is a user-determined parameter. Hence, $W_i^S(t)$ takes either zero or one depending on the value of $d_i(t)$ and becomes one for a high $d_i(t)$ value. Only discrete-time oscillators such that $W_i^S(t) = 1$ can generate oscillatory responses. For example, as illustrated in Figure 1, the first, second, eighth, and ninth oscillators generate oscillatory responses because the corresponding pixels are not black that means high pixel values. The fourth term at the right hand side of (1) is the input from the global inhibitor and Wz represents the time-invariant coupling weight. The global inhibitor described in (3) detects whether or not one or more oscillators are in high level and suppresses the levels of all oscillators if such oscillators are detected.

The i^{th} oscillator can be coupled with its neighboring oscillators. $C_i^x(t)$ and $C_i^y(t)$ in (1) and (2) express inputs from neighboring oscillators and these are defined as

$$C_i^x(t) = \rho \frac{w_{ji}(t)}{M_i(t)} \sum_{j \in L_i(t)} (x_j(t) - x_i(t)) \tag{5}$$

$$C_i^y(t) = \rho \frac{w_{ji}(t)}{M_i(t)} \sum_{j \in L_i(t)} (y_j(t) - y_i(t)) \tag{6}$$

where $w_{ji}(t)$ denotes the time-variant coupling strength from the i^{th} oscillator to the j^{th} one. Depending on the values of the i^{th} and j^{th} pixels degraded by a posterization system that is described later, the value of $w_{ji}(t)$ changes so that it becomes large when the two posterized pixel values are similar. $L_i(t)$ and $M_i(t)$ in (5) and (6) correspond to the set of neighbor oscillators having similar values of posterized pixels and the number of elements in $L_i(t)$. Note that if $M_i(t) = 0$ then we set $w_{ji}(t) / M_i(t) = 0$.

Since the couplings between neighboring oscillators become strong when the values of posterized pixels are similar, their oscillatory responses are gradually synchronized in phase. This indicates that pixels with similar values form an image region. For example, in Figure 1, the responses of the first and second oscillators are synchronized in phase; those of the eighth and ninth oscillators are also synchronized in phase.

The global inhibitor connected to all oscillators detects one or more oscillators being in high levels and suppresses the levels of all oscillators at the next time. As illustrated in Figure 1, for example, when the levels of the red oscillators become high at $t = t_k$, the global inhibitor also becomes high and the levels of all the oscillators are suppressed at the next time. As the results, the red and blue oscillators that are not directly connected each other are not synchronized in phase. Hence, the global inhibitor can prevent in-phase synchronization among oscillators in unconnected image regions.

Pixels with high pixel values are extracted according to responses from oscillators. In Figure 1, the image region consisting of the first and second pixels is extracted at $t = t_k$ because the levels of the red oscillators are high;. Similarly, another image region with the eighth and ninth pixels is also extracted at $t = t_{k+14}$. In this way, dynamic image segmentation is performed.

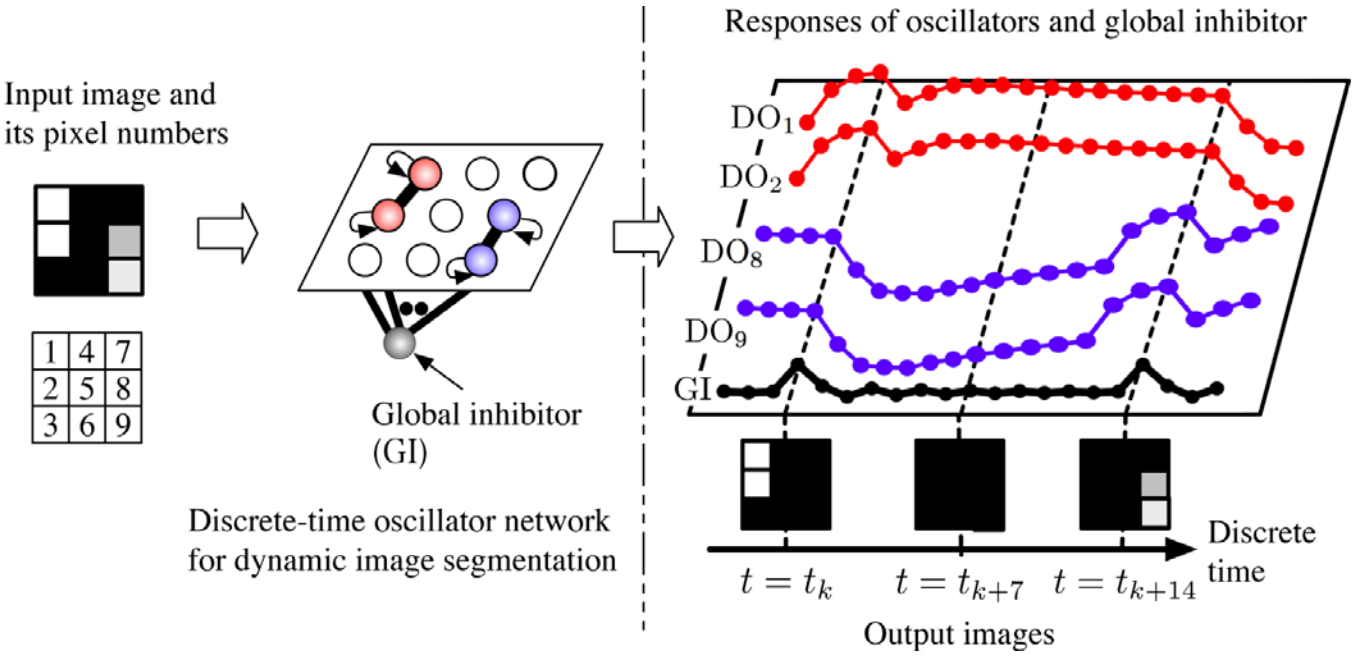

Figure 1. Schematic of dynamic image segmentation

2.2 Posterization System

The value of $d_i(t)$ is changed according to the dynamics of a posterization system. Posterization is to convert an image with a

continuous gradation of tone to several regions of fewer tones. The posterization system was modified from a discrete-time system [13].

We explain the dynamics of our posterization system and the updating of coupling strength w_{ji} in (5) and (6). Let $p_i(t)$ be the i^{th} normalized pixel value so that it takes from zero to one. The value of $p_i(t)$ is updated by the following rules:

$$p_i(t+1) = \begin{cases} 0 & \text{if } p_i(t) + \eta . F_i(t) \le 0 \\ p_i(t) + \eta . F_i(t) & \text{if } 0 < p_i(t) + \eta . F_i(t) < 1 \\ 1 & \text{if } p_i(t) + \eta . F_i(t) \ge 1 \end{cases} \tag{7}$$

where η is a parameter and

$$F_i(t) = \frac{1}{S_i(t)} \sum_{j \in \Delta_i(t)} \frac{p_j(t) - p_i(t)}{|| p_j(t) - p_i(t) ||} \exp(-\gamma || p_j(t) - p_i(t) ||) \tag{8}$$

$\Delta_i(t)$ denotes the set of pixels such that $p_j(t) \simeq p_i(t)$ in neighborhood of the ith pixel. $S_i(t)$ expresses the number of elements in $\Delta_i(t)$, but if $S_i(t) = 0$ then we set $1/S_i(t) = 0$. Whether $p_j(t) \simeq p_i(t)$, i.e., the similarity between them is measured according to the value of $q_{ij}(t)$. Its dynamics is defined as

$$q_{ij}(t+1) = \beta . q_{ij}(t) + (1-\beta) . H(\exp(-\gamma || p_j(t) - p_i(t) || \psi)) \tag{9}$$

where $H(.)$ denotes the Heaviside step function; β, γ, and ψ are parameters. According to the dynamics, the value of $q_{ij}(t)$ eventually converges to either zero or one and becomes one when $p_j(t) \simeq p_i(t)$. Hence, $\Delta_i(t)$ in (8) is redefined as the set of neighboring pixels such that $q_{ij} = 1$. The posterization of a given continuous-tone gray-scale image is performed on the basis of (7) – (9).

In (1), we set $d_i(t) = 2p_i(t)$. The coupling between the i^{th} and j^{th} oscillators is formed when the values of $q_{ij}(t)$ becomes one, i.e., $w_{ij}(t)$ becomes one. In addition, $w_{ji}(t)$ also becomes one because of symmetry coupling.

Let us illustrate the behavior of our posterization system for the 3×3 gray-scale image in Figure 2(a). The initial values $p_i(0)$, $i = 1, 2,...,9$ were set to 255, 0, 0, 230, 0, 153, 204, 0, and 64. As shown in Figure 3, the posterization system reduced the number of gray levels in the original image from five to three except black pixels after $t = 42$. As the results, the posterized image in Figure 2(b) was obtained. Moreover, since $p_i(t)$, $i = 1, 4, 7$ become similar, couplings among the first, fourth, and seventh oscillators were formed at $t = 18$ as shown in Figure 4. On the other hand, couplings between the sixth and ninth oscillators were unformed because their normalized pixel values were considerably different and these did not approach as shown in Figure 3.

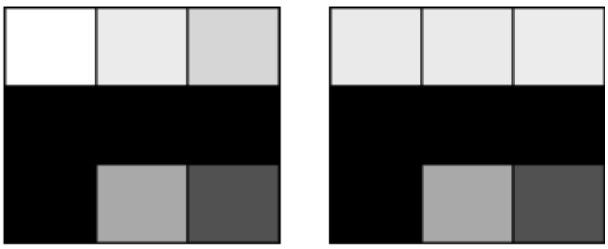

(a) original image (b) posterized image

Figure 2. 3×3 images

Oscillatory responses from the first, fourth, sixth, seventh, and ninth oscillators and the global inhibitor are plotted in Figure 5. In this simulation, the initial state values were randomly set. After couplings among the first, fourth, and seventh oscillators were formed at $t = 18$ and $p_i(t)$, $i = 1, 4, 7$ became the same at $t = 42$, the three oscillators were synchronized in phase. Moreover, the global inhibitor led to the out-of-phase synchronization of the oscillatory responses from the first, eighth, and ninth

oscillators. As the results, the oscillatory responses were able to generate three segmented image regions consisting of the first, fourth, and seventh pixels, the sixth pixel, and the ninth pixel, respectively.

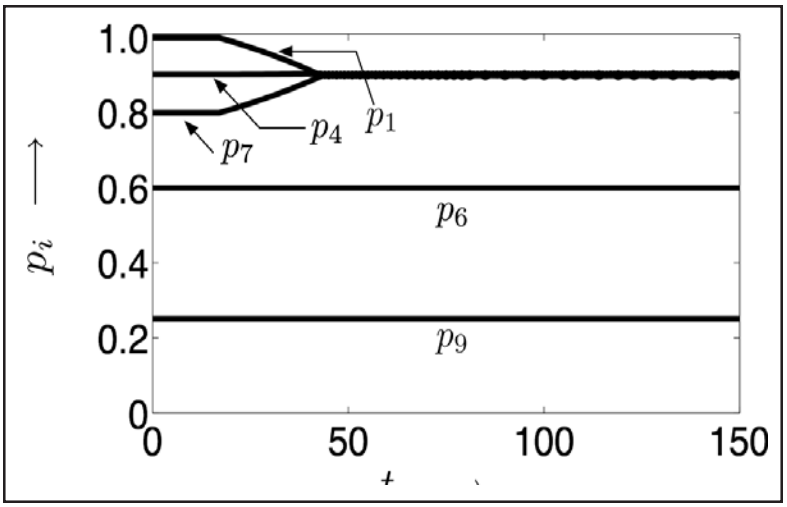

Figure 3. Posterization process

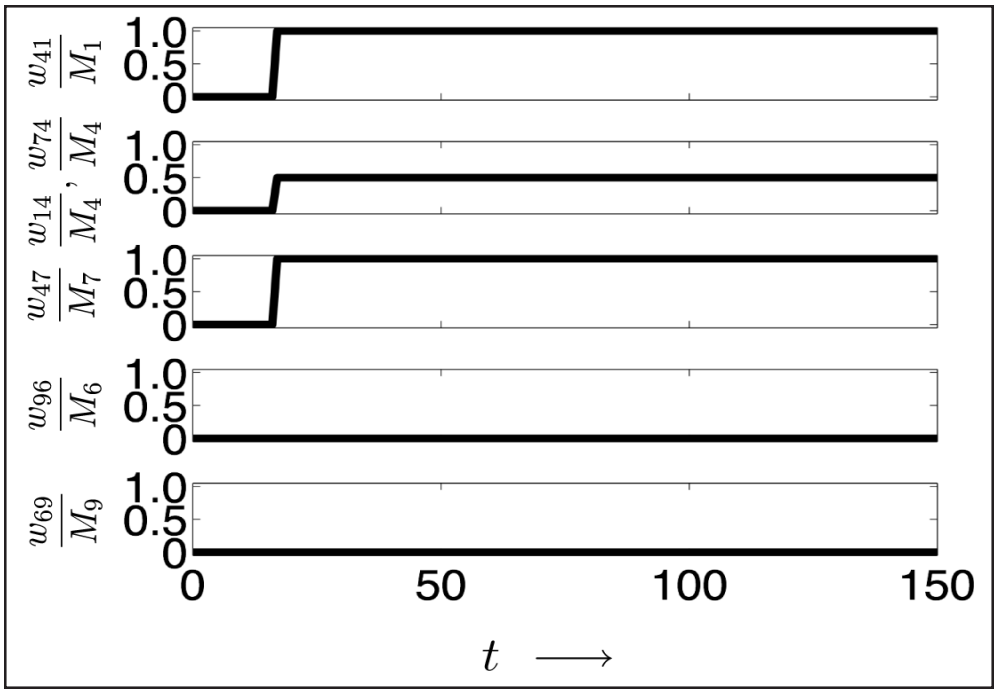

Figure 4. Time evolution of plastic couplings

3. Experimental Results and Discussion

For fast image segmentation, we implemented the proposed system into a GPU (NVIDIA Tesla C2050). Here, according to our previous analyzed results [6, 7, 8, 9], we set the system parameters in (1) – (9) except for γ to $k_f = 0.5$, $W_x = 15$, $\theta_c = 0$, $W_z = 15$, $\theta_z = 0.5$, $k_r = 0.885$, $\alpha = 4$, $a = 0.5$, $\varepsilon = 0.1$, $\phi = 0.8$, $\theta_f = 15$, $\theta_d = 0$, $\rho = 0.1$, $\psi = 0.5$, $\eta = 0.01$, and $\beta = 0.1$.

We considered segmenting of the two gray-scale images at the left of Figures 6(a) and 6(b). Here, we set $\gamma = 6.5$ and $\gamma = 5.9$ for the images in Figures 6 (a) and 6 (b), respectively. For randomly given initial state values, the proposed system output posterized

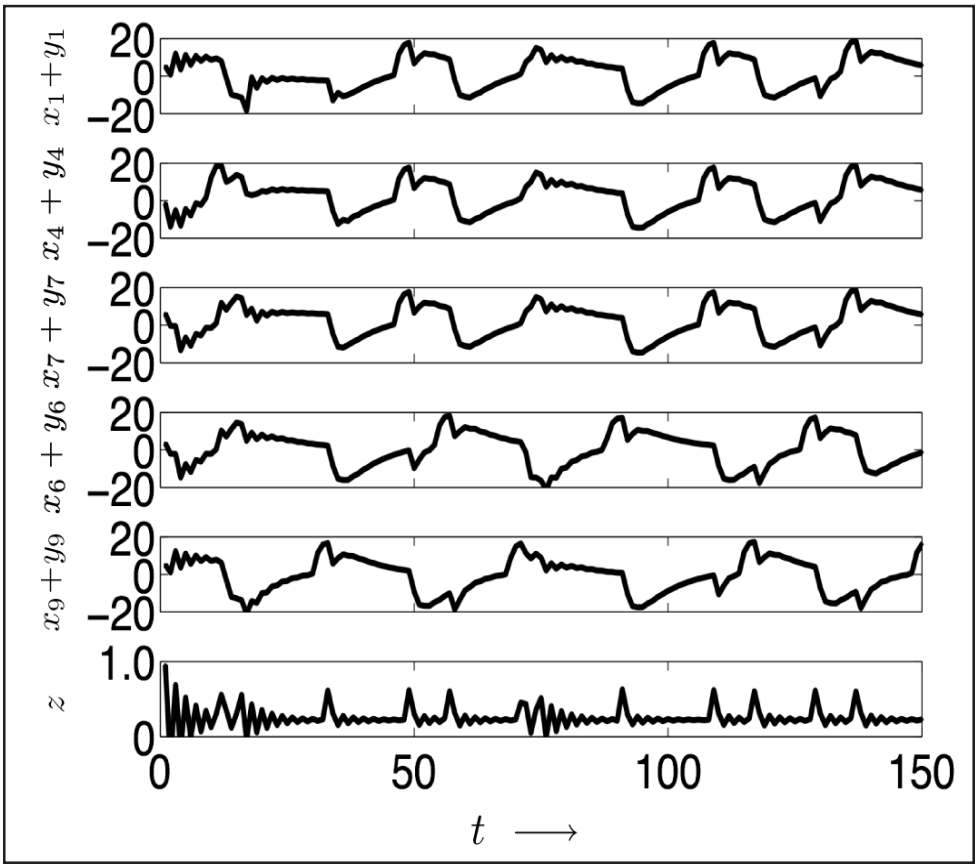

Figure 5. Time evolution of oscillatory responses

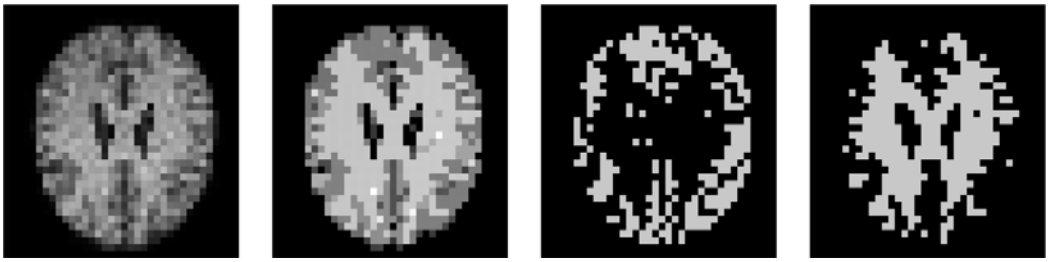

original image posterized image segmented images

(a) 36×36 image

original image posterized image segmented images

(b) 70×70 image

Figure 6. Experimental results of image segmentation

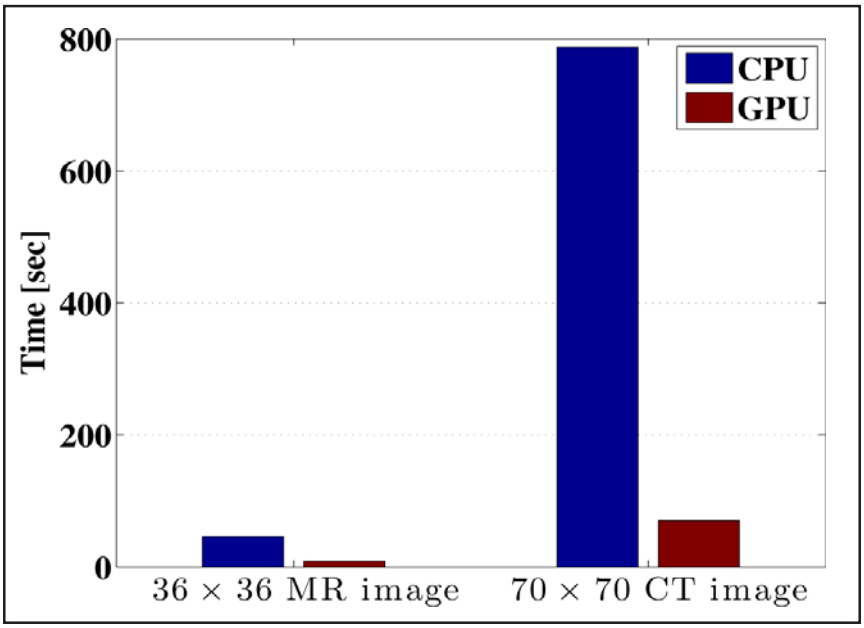

Figure 7. Comparison of processing time

images at the second column of Figure 6 after sufficient time passed. The images at the third and fourth columns of Figure 6 were picked from time-series output images of the proposed system.For ten trials for the respective original images, we measured the average time of dynamic image-segmentation processing from $t = 0$ to 500 on the GPU and a CPU (Intel Xeon W3530, 2.8 GHz). The average processing time on CPU were 45.4 seconds for the 36×36 image and 787.8 seconds for the 70×70 image. In contrast, those on GPU were 8.5 and 69.9 seconds for the 36×36 and 70×70 images, respectively. The comparison in Figure 7 indicates that the proposed system on the GPU was quite faster than that of the CPU.

4. Conclusion

We implemented our dynamic image-segmentation system into a GPU and demonstrated that the processing time of the proposed system implemented on the GPU was quite faster than that of the CPU. In addition, the proposed system produced acceptable segmented images.

References

[1] Doi, K. (2007). Computer-aided diagnosis in medical imaging: Historical review, current status and future potential. *Computerized Medical Imaging and Graphics*, 31 (4–5) 198–211.

[2] Russ, J. C. (2011). The Image Processing Handbook. CRC Press, Florida.

[3] Pal, N. R., Pal, S. K. (1993). A review on image segmentation techniques. *Pattern Recognition*, 26 (9) 1277–1294.

[4] Wang, D. L., Terman, D. (1995). Locally excitatory globally inhibitory oscillator networks. *IEEE Transactions on Neural Networks*, 6 (1) 283–286.

[5] Fujimoto, K., Musashi, M., Yoshinaga, T. (2008). Discrete-time dynamic image segmentation system. *Electronics Letters*, 44 (12) 727–729.

[6] Fujimoto, K., Musashi, M., Yoshinaga, T. (2009). Reduced model of discrete-time dynamic image segmentation system and its bifurcation analysis. *International Journal of Imaging Systems and Technology*, 19 (4) 283–289.

[7] Musashi, M., Fujimoto, K., Yoshinaga, T. (2009). Bifurcation phenomena of periodic points with high order of period observed in discrete-time two-coupled chaotic neurons. *Journal of Signal Processing*, 13 (4) 311–314.

[8] Kobayashi, M., Fujimoto, K., Yoshinaga, T (2011). Bifurcations of oscillatory responses observed in discretetime coupled neuronal system for dynamic image segmentation. *Journal of Signal Processing*, 15 (2) 145–153.

[9] Fujimoto, K., Kobayashi, M., Yoshinaga, T. (2011). Discrete-time dynamic image-segmentation system. *In*: Discrete time systems, M. A. Jordán and J. L. Bustamante (Eds.). INTECH, Rijeka, p. 405–424.

[10] Fujimoto, K., Kobayashi, M., Yoshinaga, T. (2011). Discrete-time dynamic image segmentation based on oscillations by destabilizing a fixed point. *IEEJ Transactions on Electrical and Electronic Engineering* (*TEEE*) 6 (5) 468–473.

[11] Fujimoto, K., Kobayashi, M., Yoshinaga, T., Aihara, K. (2013). Identification of target image regions based on bifurcations of a fixed point in a discrete-time oscillator network. *International Journal of Innovative Computing*, Information and Control 9 (1) 355–363.

[12] Fujimoto, K., Kobayashi, M., Yoshinaga, T. (2012). Coupled neuronal system with plastic coupling for dynamic image segmentation. *In*: 5th European Conference of the International Federation for Medical and Biological Engineering, A. Jobbágy (Ed.). IFMBE Proceedings, 37. Springer, Berlin, Heidelberg, p. 643–646.

[13] Zhao, L., Furukawa, R. A., Carvalho, A. C. P. L. F. (2003). A network of coupled chaotic maps for adaptive multi-scale image segmentation. *International Journal of Neural Systems*, 13 (2) 129–137.

[14] Fujimoto, K., Musashi, M., Yoshinaga, T. (2011). FPGA implementation of discrete-time neuronal network for dynamic image segmentation. *IEEJ Transactions on Electronics, Information and Systems*, 131 (3) 604–605.